




# Definition of a Walking with Starting and Stopping Motions for the Humanoid Romeo

A. Kalouguine<sup>1,2</sup><sup>a</sup>, V. de-León-Gómez<sup>1</sup>, C. Chevallereau<sup>1</sup><sup>b</sup>, S. Dalibard<sup>2</sup><sup>c</sup> and Y. Aoustin<sup>1,\*</sup><sup>d</sup>

<sup>1</sup>Laboratoire des Sciences du Numérique de Nantes, CNRS UMR 6004, Ecole Centrale de Nantes, Université de Nantes, France

<sup>2</sup>SoftBank Robotics, 43, Rue du Colonel Pierre Avia, 75015, Paris, France


**Keywords:** Humanoid Robot, Starting Motion, Stopping Motion, Center of Mass, Zero Moment Point, Essential Model.


**Abstract:** The aim of this paper is to develop a complete walking with a starting, periodic and stopping motion for a 3D humanoid robot with  $n$  actuated variables. The dynamic behaviour of the center of mass of the humanoid robot is defined by a model called *Essential model*. The ZMP is imposed, the horizontal position of the CoM is free. The  $n - 2$  other generalized variables of the humanoid robot are controlled and their trajectories can be for example chosen as a sinusoidal function of time. The gait parameters are determined based on data obtained from human walking. Numerical tests are presented for a complete walking motion. The perspectives are to test the obtained trajectories experimentally.


## 1 INTRODUCTION


Designing a walking trajectory for a humanoid robot entails strong difficulties such as unilateral constraints with the ground, numerous joints, respecting the dynamic equilibrium, among others. There exist several popular methods, which are based on the relation between the zero moment point (ZMP) and the center of mass (CoM), to develop walking trajectories for experiments with humanoid robots, for example (Kajita et al., 2014), (Kaneko et al., 2004). Their main advantage is to not require a lot of information about the dynamic behavior of each of the robot's bodies. However during a walking, an important flexion of the knee joint for the stance leg is actually not human-like. Also, the results are based on a simplified model, thus the walking stability is not ensured for a robot with small feet. With the linear inverted pendulum (LIP) model, walking motions based on capture point regulation are developed in order to exploit the natural dynamic of the pendulum to stop it. The capture point is the location on the ground where a biped needs to step in order to come to a stop. The CoM motion freely converges to the capture point, see (En-

glsberger et al., 2001) and (Pratt et al., 2012). But its theoretical concept is mainly based on the assumption that the altitude of the CoM is constant, *i.e.* the linear inverted pendulum (LIP) assumption. A walking gait based on human-like virtual constraints has been investigated in (Ames et al., 2012) for the robot Nao; Sakka in (Sakka, 2017) also performed this type of study for an online human motion imitation with Nao for slow motions. Another approach employed to generate walking patterns for biped robots is based on central pattern generators (CPGs) and does not require any physical model of the biped; see (Behnke, 2006), (Graf et al., 2009) or (Shachykov, 2019). However they request the tuning of a lot of parameters. The parametric optimisation can also be used to define offline walking trajectories for humanoid robots, for example (Bessonnet et al., 2002), (Tlalolini et al., 2010), or (Ames et al., 2012). The main advantage of parametric optimization is that energy consumption can be minimized. But this method requests a lot of computation efforts. The reference motion of the biped can also be based on a record of human motion (Powell et al., 2013), (Tomic et al., 2014). By definition, a human is a perfect model to define a humanoid walking. Nevertheless, making the correlation between the human motion and the robot joints is not so easy. Despite these interesting contributions, to our best knowledge there are few papers about the design of a complete walking motion, taking into ac-

<sup>a</sup> <https://orcid.org/0000-0003-3092-9534>

<sup>b</sup> <https://orcid.org/0000-0002-1929-5211>

<sup>c</sup> <https://orcid.org/0000-0001-8655-8619>

<sup>d</sup> <https://orcid.org/0000-0002-3484-117X>

\*Corresponding author

count the constraints on ZMP trajectory, with a starting, a periodic and a stopping motion. An interesting investigation was done in (Ames, 2014) but the approach was more hybrid, without double support phases. In (Khusainov et al., 2017), desired foot positions of the humanoid robot are generated for any given trajectory by taking into account kinematic limits in robot legs. In but to our best knowledge for humanoid robots there are no extract trajectories from human data.

The contribution of this paper is to fill this gap. Our main objective is to find feasible walking trajectories for a given robot, taking into account these dynamic characteristic, *i.e.* with unilateral ground contact forces and ensure dynamic equilibrium. Moreover, the proposed trajectories are inspired by average human motion, copying a particular human gait, chosen to translate an emotion like joy or fatigue, or dedicated to a task like carrying loads, etc. A complete walking motion is defined for Romeo, a humanoid robot with  $n = 31$  joints. This complete walking, which is composed of double support (DS) and single support (SS) phases is calculated by using the *Essential model*, which models the relation between ZMP and CoM by considering the complete dynamic of the robot unlike the LIP model, *i.e.* a determining feature of human gait, (De-León-Gómez et al., 2019). Vukobratovic (Vukobratovic et al., 2012) enlighten us on biomechanical inspiration of this feature to carry out biped robot motion such as posture realization, gait synthesis. The trajectory of the ZMP is here imposed, the horizontal position of the CoM of the humanoid robot is free to adapt to the ZMP evolution. The  $n - 2$  remaining generalized coordinates are given functions of time (often sinusoidal functions), whose parameters are inspired by data extracted from human walking. The CoM is thus computed from the knowledge of the evolution of the ZMP and these  $n - 2$  remaining generalized coordinates. The  $n$  joint variables of the robot are deduced from this calculation. From the inverse dynamic model it is possible to deduce the torques to carry out this complete walking.

The paper is outlined as follows. The humanoid robot Romeo is described in section 2. The *Essential model* is presented in section 3. The boundary value problem to obtain a periodic walking motion is stated in section 4. The starting and stopping phases are detailed in section 5. The results of the numerical tests are presented in section 6. Section 7 offers our conclusions and perspectives.

## 2 ROMEO

The humanoid robot considered in this study is Romeo, a prototype platform developed by the company Softbank Robotics, see fig. 1 a). It is 1.47m tall, weighs 36 kg and features 31 degrees of freedom (DoF) gathered into the configuration vector  $q$ .

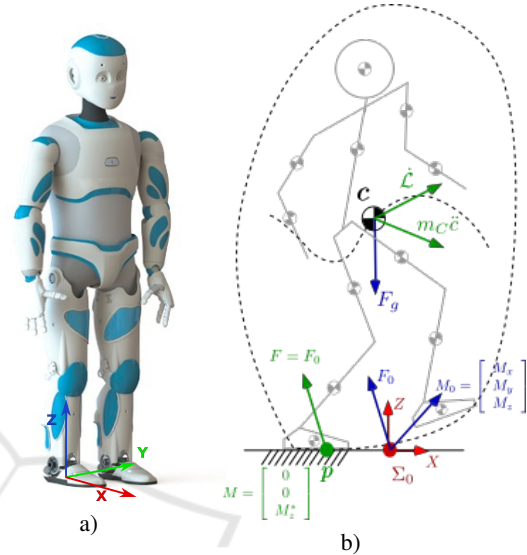


Figure 1: A) Photography of Romeo. b) Illustration of the global equilibrium.

## 3 ESSENTIAL MODEL

The objective of the *Essential model* is, instead of imposing as many trajectories as there are degrees of freedom (DoFs), to leave two DoFs free to allow for a chosen placement of the ZMP. Since the relation between ZMP and CoM is considered as a determining feature of human gait (Kajita et al., 2014), (Koolen et al., 2012), and the positions of CoM and ZMP are strongly linked, we choose to "set free" the horizontal coordinates  $r_f = (x, y)$  of the CoM in order to adapt to the imposed trajectory of the ZMP.

In order to take inspiration from the human motion, let us introduce  $r \in \mathbb{R}^{31 \times 1}$ :

$$\begin{aligned} r &= (r_f, r_c)^\top \\ &= (x, y, z(t), x_f(t), y_f(t), z_f(t), \psi_f(t), \theta_f(t), \\ &\quad \phi_f(t), \psi_t(t), \theta_t(t), \phi_t(t), q_{13}(t), \dots, q_{31}(t))^\top. \end{aligned} \quad (1)$$

We define  $r_c$  as the vector of the 29 variables of  $r$  for which the trajectories are imposed.  $z(t)$  defines the desired altitude of the CoM.  $x_f(t), y_f(t), z_f(t)$  and  $\psi_f(t), \theta_f(t), \phi_f(t)$  describe the desired position and orientation of the free foot, and  $\psi_t, \theta_t, \phi_t$  give the desired orientation of the torso link. The upper-body

variable joints are defined by  $q_{13}$  to  $q_{31}$ . The desired trajectory for  $r_c(t)$  is defined based on human motion.

The robot configuration can be defined by the joint vector  $q \in \mathbb{R}^{31 \times 1}$  or by the vector  $r$ , and a geometric model can be built. Let  $q = g(r_f, r_c)$  be,  $\dot{q}$  and  $\ddot{q}$  are deduced thanks to the kinematic models as follows:

$$\dot{q} = J_f \dot{r}_f + J_c \dot{r}_c, \quad \ddot{q} = J_f \ddot{r}_f + \dot{J}_f \dot{r}_f^2 + J_c \ddot{r}_c + \dot{J}_c \dot{r}_c^2. \quad (2)$$

Here  $J_f \in \mathbb{R}^{31 \times 2}$  and  $J_c \in \mathbb{R}^{31 \times 29}$ . In this study the evolution of  $r_c$  is chosen as a function of time, thus the joint evolution can be expressed as function of  $r_f, \dot{r}_f, \ddot{r}_f$  and  $t$  only :

$$q = g(r_f, t), \quad \dot{q} = J_f \dot{r}_f + v(t, r_f), \quad (3)$$

$$\ddot{q} = J_f \ddot{r}_f + \dot{J}_f \dot{r}_f^2 + a(t, r_f, \dot{r}_f).$$

To assess the feasibility of a walking trajectory, it is necessary to calculate the external forces acting on the humanoid robot. These external forces here are the gravity force  $F_g$  and the ground reaction forces applied on each foot (see fig. 1 b). The resulting ground reaction is defined by the wrench  $\in \mathbb{R}^{6 \times 1}$   $(F_0, M_0)^\top = (F_x, F_y, F_z, M_x, M_y, M_z)^\top$  in a reference frame  $\Sigma_0$ . The global equilibrium of the robot can be written as :

$$\begin{pmatrix} F_0 \\ M_0 \end{pmatrix} = \begin{pmatrix} A_F \\ A_M \end{pmatrix} \ddot{q} + \begin{pmatrix} d_F(q, \dot{q}) \\ d_M(q, \dot{q}) \end{pmatrix} \quad (4)$$

where  $q \in \mathbb{R}^{31 \times 1}$  is the joint vector of the robot.

Using (3), the global equilibrium (4) can be rewritten:

$$\begin{pmatrix} F_0 \\ M_0 \end{pmatrix} = \begin{pmatrix} A_{Fr}(t, r_f) \\ A_{Mr}(t, r_f) \end{pmatrix} \ddot{r}_f + \begin{pmatrix} d_{Fr}(t, r_f, \dot{r}_f) \\ d_{Mr}(t, r_f, \dot{r}_f) \end{pmatrix} \quad (5)$$

Let  $p = (p_x, p_y, 0)^\top$  be the global zero moment point (ZMP). Its coordinates  $p_x$  and  $p_y$  satisfy :

$$F_z p_x + M_y = 0, \quad F_z p_y - M_x = 0. \quad (6)$$

$(p_x, p_y)$  must be inside the convex hull of support at all times in order to satisfy the dynamic equilibrium condition (Vukobratovic and Borovac, 2004). We impose a desired evolution of the ZMP  $p_x(t)$  and  $p_y(t)$  inside the convex hull of the support foot (or feet in DS) in order to satisfy the equilibrium condition. During the SS phase the desired motion of the ZMP is a migration of the ZMP from the heel to the toe of the stance foot. In DS phase the desired motion of the ZMP is defined by a linear evolution from the final position of the ZMP at the end of the SS phase on the stance foot, until the initial position of the ZMP at the beginning of the SS on the next stance foot. By using the 3<sup>th</sup>, 4<sup>th</sup>, and 5<sup>th</sup> lines of (5), we rewrite (6) as:

$$\begin{aligned} & (A_{Frz}(t, r_f) \ddot{r}_f + d_{Frz}(t, r_f, \dot{r}_f)) p_x(t) + \\ & A_{Mry}(t, r_f) \ddot{r}_f + d_{Mry}(t, r_f, \dot{r}_f) = 0, \quad (7) \\ & (A_{Frz}(t, r_f) \ddot{r}_f + d_{Frz}(t, r_f, \dot{r}_f)) p_x(t) - \\ & A_{Mrx}(t, r_f) \ddot{r}_f - d_{Mrx}(t, r_f, \dot{r}_f) = 0. \end{aligned}$$

These two scalar equations (7) isolate the essential characteristic of the walking that is the relationship between the ZMP and the CoM. Solving (7) gives the *Essential model* describing the acceleration of the horizontal positions  $x$  and  $y$  of the CoM, that are defined to achieve the imposed evolution of the ZMP:

$$\ddot{r}_f = f(r_f, \dot{r}_f, t, p_x(t), p_y(t)). \quad (8)$$

By integration of (8) from initial conditions we can calculate the current values of  $\dot{r}_f$ , i.e.  $\dot{x}$ ,  $\dot{y}$ , and  $r_f$ , i.e.  $x$ , and  $y$ . To sum up, the evolution of  $x$  and  $y$  is not imposed in order to allow them to adapt to the imposed evolution of the ZMP. With this strategy to define a reference trajectory of walking, which is based on the *Essential model* (8) and  $r_c(t)$ , no approximations are made to the dynamic model when designing the humanoid walking. The method ensures the feasibility of a walking trajectory from the point of view of the condition on the ZMP.

The choice of the height  $z(t)$  of the CoM allows to satisfy the positivity of the vertical component of the resultant ground reaction force during the walking. It is sufficient to satisfy

$$\ddot{z}(t) > -g$$

The condition of no slipping can be checked based on the knowledge of  $\ddot{r}_f$  and  $\ddot{z}$ . It is sufficient to satisfy

$$\|\ddot{r}_f(t)\| < \mu(\ddot{z}(t) - g)$$

where  $\mu$  is the friction coefficient. The numerical validation of these conditions is presented in fig. 9.

### 3.1 Torques and Ground Forces in SS and DS

By now, the torques required to produce the motion have to be calculated. During the SS phase, by considering the stance foot motionless on the ground, we can define the dynamic behavior of the robot:

$$\tau = A_r(t, r, f) \ddot{r}_f + d_r(t, r_f, \dot{r}_f) \quad (9)$$

In DS phase, the effort wrench  $(F_{ext}, M_{ext})^\top$  applied on the second leg, (9) becomes

$$\tau = A_r(t, r_f) \ddot{r}_f + d_r(t, r_f, \dot{r}_f) + J_{ext} \begin{pmatrix} F_{ext} \\ M_{ext} \end{pmatrix}. \quad (10)$$

The global equation gives the global reaction effort  $F_0, M_0$ , but the distribution on both legs is free and will modify the actuation torque. During a DS, the global ZMP is the barycentre of the two local ZMPs on each foot, this implies that the global ZMP and the local ZMPs are aligned. In DS, the choice of local ZMPs  $p_1$  and  $p_2$  is used to calculate the distribution

of efforts. This choice must limit the internal forces useless to the motion in order to avoid increasing the joint torques. We can then calculate the vertical reaction force  $F_{1z}$  and  $F_{2z}$  on legs 1 and 2 by solving this system:

$$\begin{aligned} \frac{p_{1x}F_{1z} + p_{2x}F_{2z}}{F_{1z} + F_{2z}} &= p_x \\ \frac{p_{1y}F_{1z} + p_{2y}F_{2z}}{F_{1z} + F_{2z}} &= p_y \end{aligned} \quad (11)$$

To limit the risk of slipping, the ratio between tangential and normal forces for the global equilibrium is chosen equal for each leg. The components  $F_{1x}$ ,  $F_{1y}$ ,  $F_{2x}$ , and  $F_{2y}$  are calculated to satisfy:

$$\begin{aligned} \frac{F_{1x}}{F_{1z}} &= \frac{F_{2x}}{F_{2z}} = \frac{F_{1x} + F_{2x}}{F_{1z} + F_{2z}} \\ \frac{F_{1y}}{F_{1z}} &= \frac{F_{2y}}{F_{2z}} = \frac{F_{1y} + F_{2y}}{F_{1z} + F_{2z}} \end{aligned} \quad (12)$$

By using (11) and (12) we find  $M_z = M_{1z} + M_{2z}$ . The moment around the  $z$  axis is also shared between the two legs by using a similar distribution to the force components (12) as follows:

$$\frac{M_{1z}}{F_{1z}} = \frac{M_{2z}}{F_{2z}} = \frac{M_{1z} + M_{2z}}{F_{1z} + F_{2z}} \quad (13)$$

In this study, two types of DS phases are considered.

- DS during the walking phase which allows to join two phases of SS with foot positions offsets along the  $x$  and  $y$  axes. We want to have a continuous evolution of the ZMP, which results in continuous joint torques and avoids high jerk. We choose an evolution of the global ZMP in order that during the DS phases, the two local ZMPs keep a constant pose corresponding to the final pose of the ZMP in SS:  $p_1$ , and the initial pose of the ZMP for the next SS:  $p_2$ . This implies that the global ZMP evolves linearly between the final pose of the ZMP during the previous SS and the initial pose of the ZMP during the next SS.
- For the initial DS in starting phase, or the final DS in stopping phase, on the contrary, we have the two feet aligned along the  $x$ -axis and a non-linear evolution of the global ZMP (Jian et al., 1993). The local ZMPs will then be chosen to yield the current value of the global ZMP along the  $x$ -axis while remaining within the surface of the corresponding foot. In addition, when stationary, we want an identical distribution of forces over the two feet, we choose a position of the CoM according to the  $y$ -direction between the two feet and a  $y$ -position of the local ZMPs in the center of the

feet. A linear ZMP evolution along the  $y$ -axis is chosen. The aim is to ensure continuity and to minimize the lateral torque on the ankle. An illustration is shown in fig. 8 for the case studied.

## 4 PERIODIC WALKING MOTION

The periodic motion is composed of SS phases and DS phases with flat foot contacts on the ground. There is no impact at the end of the SS phase, since the velocity of the swing foot is imposed to be zero when it touches the ground. A quadratic-cycloidal function is used to define the trajectory of the swing foot. The orientation of its sole is varying during motion, but parallel to the ground during DS phases. Sinusoidal functions are used to define the motions of the arms and the trunk. The parameters of these functions are tuned based on observations of human motions (Winter, 1992). To define a periodic walking motion for Romeo, the step width  $D$  and the step length  $S$  are adapted to its physical characteristics and the limits of its actuators. The step width  $D$  is chosen to be 0.20m to satisfy a safe clearance between Romeo's ankles. The step length  $S$  is chosen in the range 0.15 to 0.20m, which corresponds to a 0.30-0.40m displacement of the swing foot and a velocity of 0.83 to 1.1km/h respectively. The duration of one DS phase is chosen to be close to 12% of the cycle (2 steps) duration  $2 \cdot T$ , where  $T = T_{DS} + T_{SS}$ .  $T_{DS} = 0.15$ s and  $T_{SS} = 0.60$ s are the chosen durations of the DS phases and SS phases. In SS, the ZMP evolution is chosen as linear along the  $x$  axis and centered in the middle of the foot along the  $y$  axis. In DS, the ZMP evolves linearly between its final position in the previous SS and its initial position in the next SS as explained in section 3.1.

To find the periodic motion, a boundary value problem is stated and solved as follows. Let  $(x(t_0), y(t_0), \dot{x}(t_0), \dot{y}(t_0))$  be the components in the horizontal plane of the position and velocity of the COM at the beginning of a current step of the walking motion. The periodic condition is

$$\begin{aligned} (x(t_0), y(t_0), \dot{x}(t_0), \dot{y}(t_0)) &= \\ (x(t_0 + T), y(t_0 + T), \dot{x}^+(t_0 + T), \dot{y}^+(t_0 + T)) & \end{aligned} \quad (14)$$

by taking into account the change of the reference frame when the two legs switch their roles just at the beginning of the current step. So  $\dot{x}^+(t_0 + T), \dot{y}^+(t_0 + T)$  are the initial velocities of the COM in SS of the next step. The boundary value problem is stated as: what are  $x(t_0), y(t_0), \dot{x}(t_0)$  and  $\dot{y}(t_0)$  such that after integration of (8) over the time interval  $[t_0, t_0 + T]$  the periodic condition (14) is satisfied.

## 5 STARTING AND STOPPING MOTIONS

In order to perform the target periodic walking motion experimentally, it is necessary to add starting and stopping motions, which are composed of DS phases and SS phases. This allows the robot to start from (resp. to stop in) a resting position. Each resting position is defined to be a static equilibrium where the vertical projection of the CoM on the ground is merged with the ZMP close to the center of the convex hull of support. From the observation of data from human walking (Grundy et al., 1975) a ZMP trajectory is defined by using piecewise polynomial functions to be adapted to a humanoid robot. A sequence of starting phase ( $DS_1$ ,  $SS_1$ , and  $DS_2$ ), a periodic walking motion (SS and DS) and a stopping phase ( $SS_{n-1}$ ,  $DS_{n-1}$ ,  $SS_n$ , and  $DSS_n$ ) is shown in fig. 2.

For the starting motion control points are introduced:

- $\mathbf{P}_0$  ZMP at the start of  $DS_1$
- $\mathbf{P}_1$  ZMP in the middle of  $DS_1$
- $\mathbf{P}_2$  ZMP at the transition between  $DS_1$  and  $SS_1$
- $\mathbf{P}_3$  ZMP at the transition between  $SS_1$  and  $DS_2$
- $\mathbf{P}_4$  ZMP at the end of the  $DS_2$  phase

These control points are used to define the evolution of ZMP during starting phase. They are illustrated on fig. 2

In  $DS_1$  phase  $p_x$  and  $p_y$  are both defined as quadratic functions of time going from  $\mathbf{P}_0$  to  $\mathbf{P}_2$  with the intermediate point  $\mathbf{P}_1$ . In  $SS_1$  and  $DS_2$  phases  $p_x$  and  $p_y$  are defined as linear functions of time connecting, respectively,  $\mathbf{P}_2$  to  $\mathbf{P}_3$  and  $\mathbf{P}_3$  to  $\mathbf{P}_4$ .  $\mathbf{P}_4$  is imposed by the chosen periodic trajectory.

For the stopping motion, the strategy to define the ZMP trajectory is similar. We define:

- $\mathbf{P}_5$  ZMP at the transition between  $SS_{n-1}$  and  $DS_{n-1}$
- $\mathbf{P}_6$  ZMP at the transition between  $DS_{n-1}$  and  $SS_n$
- $\mathbf{P}_7$  ZMP at the transition between  $SS_n$  and  $DS_n$
- $\mathbf{P}_8$  ZMP in the middle of  $DS_n$
- $\mathbf{P}_9$  ZMP at the end of the  $DS_n$  phase

At the start of  $SS_{n-1}$  phase, the ZMP position is (taking into account the change of reference frame) the same as in  $\mathbf{P}_4$  because of the periodic nature of the trajectory before  $SS_{n-1}$ . We can therefore denote this point as  $\mathbf{P}_4$  as well. In  $SS_{n-1}$  phase,  $p_x$  and  $p_y$  are therefore defined as linear functions to connect  $\mathbf{P}_4$  to  $\mathbf{P}_5$ . In  $DS_{n-1}$  and  $SS_n$  phases,  $p_x$  and  $p_y$  are defined as

linear functions of time to connect  $\mathbf{P}_5$  to  $\mathbf{P}_6$ ,  $\mathbf{P}_6$  to  $\mathbf{P}_7$ , respectively. In  $DS_n$  phase  $p_x$  and  $p_y$  are defined as quadratic functions of time connecting  $\mathbf{P}_7$  to  $\mathbf{P}_9$  with an intermediate point  $\mathbf{P}_8$ .

The stopping phase with two DS phases and two SS phases is not symmetric with respect to the starting phase with two DS phases and only one SS phase in order to mimic easier the motion of the ZMP in humans during the starting and stopping motions. The step width  $D$  and the step length  $S$  are given but not necessarily similar between the starting, stopping and periodic motions. A boundary value problem is solved to define the starting and stopping motions. This boundary value problem is stated as follows:

**Starting Motion.** Let us consider the known **two** coordinates of the horizontal position of the CoM, which is also the ZMP position  $\mathbf{P}_0$ . Their **two** velocities are equal to zero. Let us consider the known **two** coordinates of the horizontal position of the CoM at the end of  $DS_2$  phase and their **two** velocities. These two coordinates and two velocities are also the state of the periodic horizontal motion of the CoM at the beginning of the SS phase.

Let us take into account the essential model (8) and  $T_{start}$  the duration of the starting motion. What are the **four** possible variables to carry out the starting motion by integration of (8) from  $(X(0), Y(0), \dot{X}(0), \dot{Y}(0))^T$  to  $(X(T_{start}), Y(T_{start}), \dot{X}(T_{start}), \dot{Y}(T_{start}))^T$ ? We choose the components  $p_x$  and  $p_y$  of the two *control points*  $P_2$ , and  $P_3$  of the ZMP trajectory, to solve this boundary problem. A *SQP* method (Sequential Quadratic Programming) with *fmincon* of Matlab (®) is used to find the coordinates of  $P_2$ , and  $P_3$  in order to easier ensure that the ZMP is always inside of the convex hull of the support area. The *Essential model* dynamics are then integrated from the starting state  $(r_f(0), \dot{r}_f(0))^T$  for this COM, to the final state  $(r_f(T_{start}), \dot{r}_f(T_{start}))^T$  of the starting motion. This final state is compared to the target state  $(r_f^{des}(T_{start}), \dot{r}_f^{des}(T_{start}))^T$  by using a Mean Square criterion (optionally weighed to emphasize the importance of one of the dimensions):

$$J = (X(T_{start}) - X^{des}(T_{start}))^2 + (Y(T_{start}) - Y^{des}(T_{start}))^2 + (\dot{X}(T_{start}) - \dot{X}^{des}(T_{start}))^2 + (\dot{Y}(T_{start}) - \dot{Y}^{des}(T_{start}))^2. \quad (15)$$

**Stopping Motion.** The strategy is similar to that of the starting motion. For the **four** possible variables to carry out the stopping motion we choose

the components  $p_x$  and  $p_y$  of the **two control points**  $P_6$  to  $P_7$  of the ZMP trajectory, to solve this boundary problem. An equivalent criterion to (5) is calculated with respect to the **two** coordinates of the horizontal resting position of the CoM and their **two** respective velocities.

$$J = (X(T_{stop}) - X^{des}(T_{stop}))^2 + (Y(T_{stop}) - Y^{des}(T_{stop}))^2 + \dot{X}(T_{stop})^2 + \dot{Y}(T_{stop})^2. \quad (16)$$

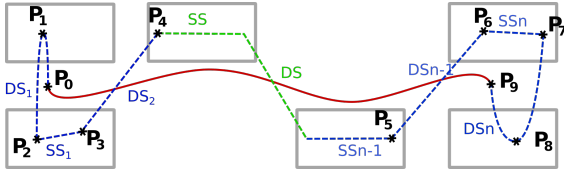


Figure 2: Sequence starting motion, cycling walking stopping motion.

All joint trajectories also need to be continuous during this transition. And since there is no impact in our gait, this is equivalent to imposing that the evolution of  $r_c$  be continuous. The sinusoidal functions, which define the actuated joints of the arms and trunk, are multiplied by a piecewise polynomial cut-off function which is equal to 1 during the periodic motion and smoothly goes to 0 during the starting and stopping phases in order to start and to stop with a null velocity and null acceleration.

## 6 NUMERICAL RESULTS

### 6.1 Periodic Motion

We choose a ZMP trajectory close to the one that is observed in humans. Since we do not have foot roll-off motion, we avoid the ZMP reaching the edges of the foot. That way, the non-tilting condition is safely satisfied.

The evolution of ZMP in DS phase is chosen as follows:

- In  $x$ -direction, from  $p_x = 0$  (under the ankle) to  $p_x = 0.10\text{m}$  (in the toes of the foot).
- In  $y$ -direction,  $p_y = 0$  (center of the foot).

The corresponding COM trajectory is represented on fig. 3. We observe that the COM trajectory in the horizontal plane is not far from a sinus function, which is what is observed for humans (Rose and Gamble, 2006).

However, when calculating the torque values for this trajectory, we observe that the torques are not

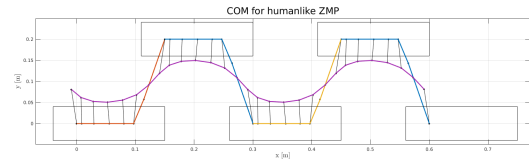


Figure 3: COM trajectory corresponding to a human-like evolution of the ZMP.

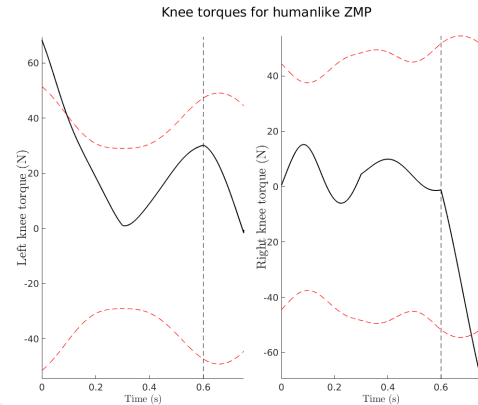


Figure 4: Torques at both knees for a human-like ZMP trajectory. The dashed line marks the end of the SS phase (swing foot contact), and the red dashed lines show the maximum acceptable torque for Romeo. It is interesting to note that these limits are not constant - this is because of a specificity of the knee joint in Romeo: the maximum torque depends on the joint position.

compatible with the hardware of Romeo, as shown in fig. 4. In order to reduce these torques, we need to make some adaptations to the original parameters. We analyzed the effect of various parameters on the torques, and observed that the most efficient way to influence the knee torques is to modify the ZMP trajectory. The result of this adaptation is presented in the following section, and the trajectory used in the rest of the paper is the modified one.

### 6.2 Effect of ZMP Evolution on Torques

The results presented above correspond to an evolution of the ZMP going from the heel to the tip of each foot (see fig. 3). The torque at the ankle is directly affected by the pose of the ZMP. It can be seen in fig. 5 (2<sup>nd</sup> image), that the propulsive torque at the ankle is low at the beginning of the step. As a consequence, a high propulsive torque is required at the knee joint (fig. 5 (3<sup>th</sup> image)). In fact this high torque exceeds the limits of the actuator (shown in dotted line) of the robot Romeo. We explored the effect of the influence of ZMP evolution. The results show that a modification of the ZMP trajectory influences the torques in the support knee and in the support ankle. A ZMP

that has a constant position in front of the foot allows a higher propulsive force in the ankle at the beginning of the SS, and thus allows to decrease the propulsive force at knee, and then produces a knee torque compatible with the actuator of Romeo.

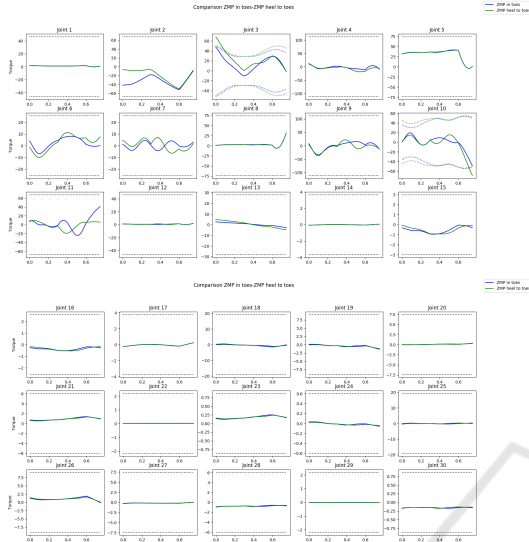


Figure 5: Joint torques (N.m) versus time (s): comparison of the torque in the lower part of the robot for two periodic trajectories with a step size of 0.20 m and a period of 0.75 s. The trajectory in green is with a human like ZMP evolution in DS, and the trajectory in blue has a ZMP constrained to the front of the foot.

### 6.3 Complete Motion

The synthesised walking trajectory is such that the step width parameter  $D$  is the same for the starting, periodic and stopping motions. The step length parameter  $S$  is chosen to be 0.16m, 0.15m and 0.20m for the starting, periodic and stopping motions respectively. For this synthesised trajectory, the trajectories of the horizontal position of the CoM and the ZMP are shown fig. 6. The starting motion and the stopping phases are respectively composed of three and four phases. Four steps make up the periodic motions. During this periodic motion the step size equals 0.15m. We can observe that the COM and ZMP evolutions are continuous from the starting configuration to the stopping configuration.

A focus of the starting and stopping phases is presented fig. 7. The horizontal position of the CoM and the ZMP position coincide well at the starting and stopping configurations. The control points to solve the two boundary value problems are depicted with green stars.

In the first and last DS phases, the ZMP follows a more complex trajectory. It is therefore necessary

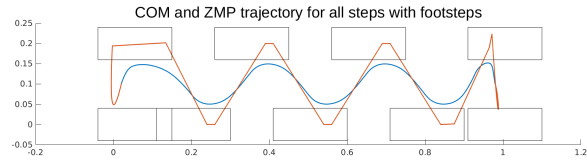


Figure 6: Imposed ZMP trajectory (orange) and corresponding COM (blue). The dashed rectangles represent the foot placements.

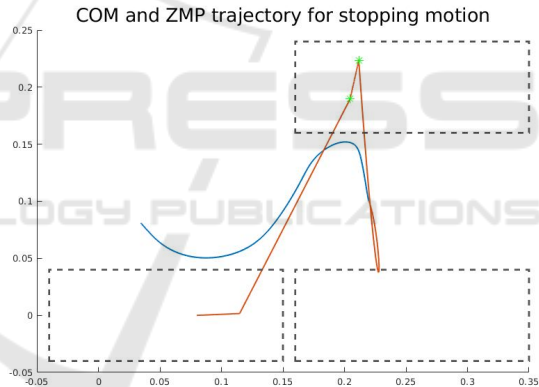
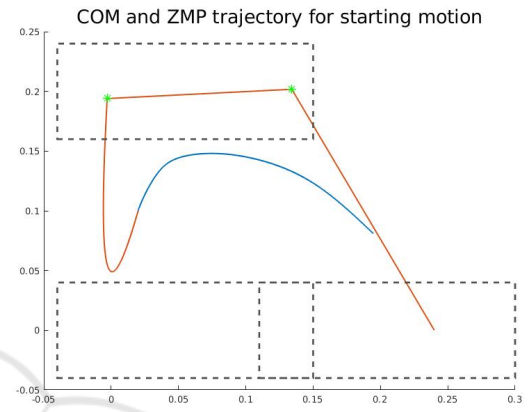


Figure 7: Imposed ZMP trajectory (orange) and horizontal position of the corresponding COM (blue).

to define a non constant local ZMP for each foot. We choose at all times to keep the same  $x$  coordinate as the global ZMP, and stay as close as possible to the center of each foot in  $y$  direction to improve walking stability. The resulting local ZMP trajectories are presented in fig. 8.

We can also verify that the non slipping condition is fulfilled. This condition is the fact that the ratio between the tangential and normal forces does not exceed the friction coefficient. This friction coefficient is chosen equal to 0.7 here. Both of these forces are calculated with (4). The sinusoidal-like shape of the normal reaction force observed in fig. 9 is linked to the oscillations of the height  $z$  the COM  $F = m\ddot{z} + mg$ .

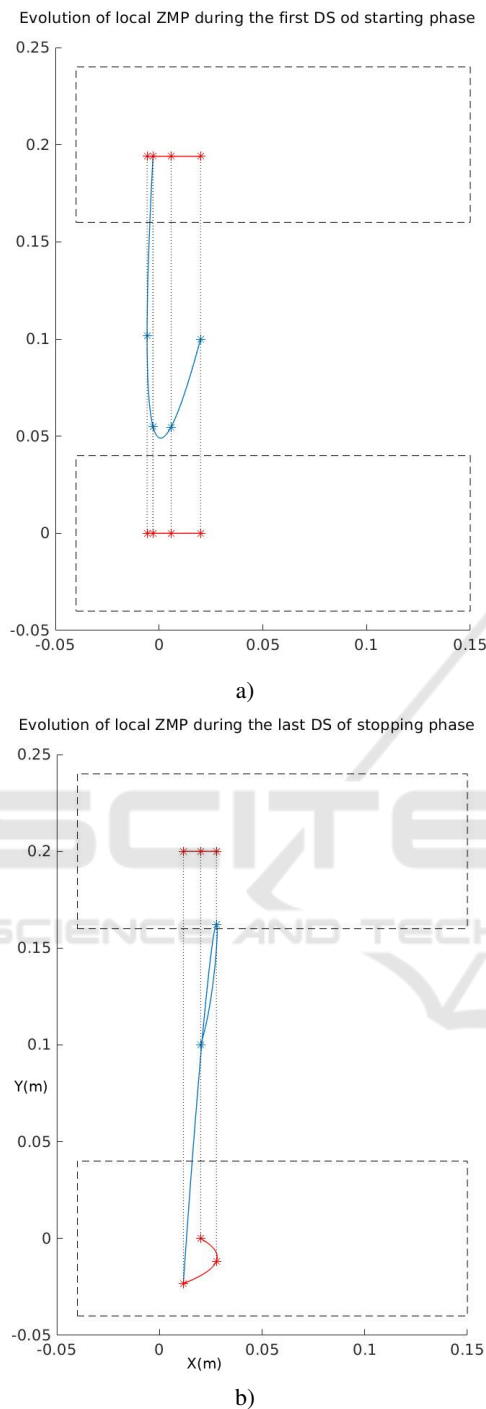


Figure 8: Evolution of the local ZMP (red) for each foot respectively during the first and last DS phases of the starting (a) and stopping (b) motions. The blue line indicates the corresponding COM evolution, resp. starting and stopping in the middle of both feet. The dashed lines show the distribution of the global ZMP and its relation to the COM position.

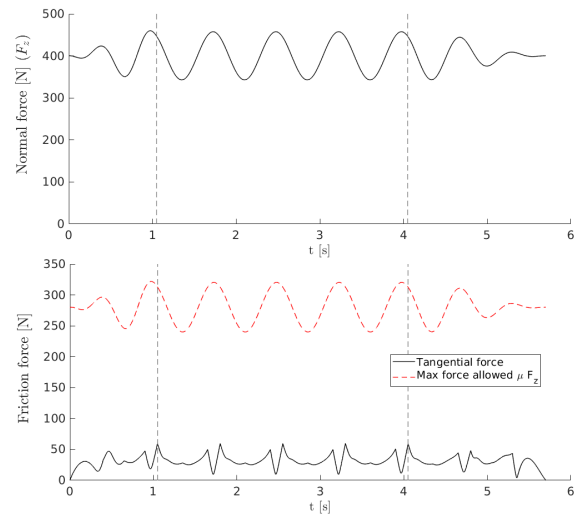


Figure 9: Normal (top plot) and tangential (bottom) components of the reaction force. The red dashed line represents the maximum acceptable tangential force without risk of slipping.

We compute the torque value for all of the joints. However, we choose to only present in fig. 10 the torques on both legs in the joints in the sagittal plane. Indeed, these are the torques that require the highest magnitude. It can be observed that the torques are inside to motor limits for the studied robot. The torque required for starting, periodic, and stopping motions are of similar magnitude.

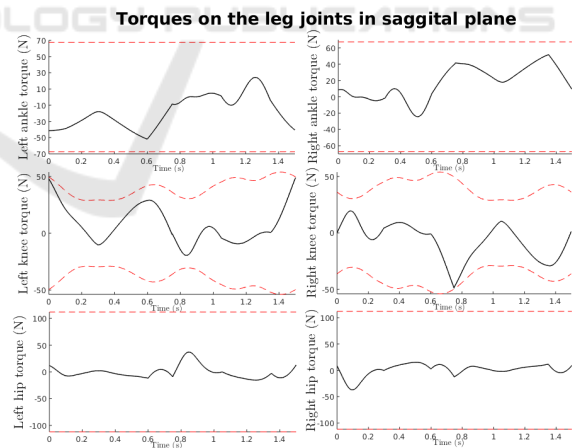


Figure 10: The torque at the ankle, knee and hip joints, in the sagittal plane for the complete motion.

## 7 CONCLUSIONS

A complete walking with a starting motion and a stopping motion is defined thanks to a strategy based on the *Essential model*. This methodology ensures the



feasibility of the walking trajectory with respect to the condition on the ground reaction force: take off, slipping and rotation of the support foot are avoided. The ZMP trajectory is ensured to be inside a convex hull of the support surface. The parameters of trajectories of the swing leg ankle, the trunk and the arms are tuned thanks to observations from human walking. The effect of the choice of the ZMP evolution on the required torque is investigated. A correlation between the pose of the ZMP in sagittal plane and torque at ankle and knee in sagittal plane has been shown. The perspectives are to test this complete walking motion experimentally.

## REFERENCES

- Ames, A. D. (2014). Human-inspired control of bipedal walking robots. *IEEE Transactions on Automatic Control*, 59(5):1115–1130.
- Ames, A. D., Cousineau, E. A., and Powell, M. J. (2012). Dynamically stable bipedal robotic walking with nao via human-inspired hybrid zero dynamics. In *Proc. of the 15th ACM int. conf. on Hybrid Systems: Computation and Control*, pages 135–144. ACM.
- Behnke, S. (2006). Online trajectory generation for omnidirectional biped walking. In *Proc. Int. Conf. on Robotics and Automation (ICRA)*, pages 1597–1603, Orlando, USA.
- Bessonnet, G., Chesse, S., and Sardin, P. (2002). Generating optimal gait of a human-sized biped robot. In *Proc. of the fifth Int. Conf. on Climbing and Walking Robots*, pages 717–724.
- De-León-Gómez, V., Luo, Q., Kalouguine, A., Pámanes, J. A., Aoustin, Y., and Chevallereau, C. (2019). An essential model for generating walking motions for humanoid robots. *Robotics and Autonomous Systems*, 112:229–243.
- Engelsberger, J., Ott, C., Roa, M. A., Albu-Shäffer, A., and Hirzinger, G. (2001). Bipedal walking control based on capture point dynamics. In *Proc. Int. Conf. on Intelligent Robots and Systems (IROS)*, pages 4420–4427, San Francisco, USA.
- Graf, C., Häryl, A., Röfer, T., and Laue, T. (2009). A robust closed-loop gait for the standard platform league humanoid. In *Proc. Workshop on Humanoid Soccer Robots of the IEEE-RAS Int. Conf. on Humanoid Robots*, pages 30–37, Paris, France.
- Grundy, M., Tosh, P., McLeish, R., and Smidt, L. (1975). An investigation of the centres of pressure under the foot while walking. *J. of bone and joint surgery. British volume*, 57(1):98–103.
- Jian, Y., Winter, D. A., Ishac, M. G., and Gilchrist, L. (1993). Trajectory of the body cog and cop during initiation and termination of gait. *Gait & Posture*, 1(1):9–22.
- Kajita, S., Hirukawa, H., Harada, K., and Yokoi, K. (2014). *Introduction to humanoid robotics*, volume 101. Springer.
- Kaneko, K., Kanehiro, F., Kajita, S., Hirukawa, H., Kawasaki, T., Hirata, M., K.Akachi, and Isozumi, T. (2004). Humanoid robot hrp-2. In *Proc. IEEE Int. Conf. on Robotics and Automation ICRA*, pages 1083–1090, New-Orleans, Louisiana, USA.
- Khusainov, R., Sagitov, A., Klimchik, A., and Magid, E. (2017). Arbitrary trajectory foot planner for bipedal walking. In *ICINCO (2)*, pages 417–424.
- Koolen, T., de Boer, T., Rebula, J., Goswami, A., and Pratt, J. (2012). Capturability-based analysis and control of legged locomotion, part 1: Theory and application to three simple gait models. *Int. J. of Robotics Research*, 31(09):1094–1113.
- Powell, M. J., Heraeid, A., and Ames, A. D. (2013). Speed regulate in 3d robotic walking through motion transitions between human-inspired partial hybrid zero dynamics. In *Proc. IEEE Int. Conf. on Robotics and Automation (ICRA)*, pages 4803–4810, Karlsruhe, Germany.
- Pratt, J. E., Koolen, T., de Boer, T., Rebula, J. R., Cotton, S., Carff, J., Johnson, M., and Neuhaus, P. D. (2012). Capturability-based analysis and control of legged locomotion, part 2: application to m2v2, a lower-body humanoid. *The International Journal of Robotic Research*, 31(10):1117–1133.
- Rose, J. and Gamble, J. G. (2006). *Human walking*. Williams & Wilkins, 3 edition.
- Sakka, S. (2017). *Imitation des mouvements humains par un robot humanoïde sous contrainte d'équilibre*. HDR, Université Pierre et Marie Curie (UPMC).
- Shachykov, A. (2019). *Biomedical signals analysis and neural modeling of motor coordination in Parkinson's disease*. PhD thesis, Université de Lorraine France.
- Tlalolini, D., Aoustin, Y., and Chevallereau, C. (2010). Design of a walking cyclic gait with single support phases and impacts for the locomotor system of a thirteen-link 3d biped using the parametric optimization. *Multibody System Dynamics*, 23(1):33–56.
- Tomic, M., Vassallo, C., Chevallereau, C., Rodic, A., and Potkonjak, V. (2014). Arms motion of a humanoid inspired by human motion. In *Proc. Int. Conf. Medical and Service Robotics (MESROB 2014)*, Lausanne, Switzerland.
- Vukobratovic, M. and Borovac, B. (2004). Zero-moment point-thirty five years of its life. *Int. J. of Humanoid Robotics*, 1(1):157–173.
- Vukobratovic, M., Borovac, B., Rodic, A. and, K. D., and Potkonjak, V. (2012). A bio-inspired approach to the realization of sustained humanoid motion. *Int. J. of Advanced Robotic System*, 9(201):1–16.
- Winter, D. A. (1992). Foot trajectory in human gait: a precise and multifactorial motor control task. *Physical therapy*, 72(1):45–53.